



INTERNATIONAL ATOMIC ENERGY AGENCY

INDC(NDS)-0475

Distr. AC

I N D C INTERNATIONAL NUCLEAR DATA COMMITTEE

Status of Thermal Neutron Scattering Data for Graphite

M. Mattes and J. Keinert

Institute for Nuclear Technology and Energy Systems (IKE) – University of Stuttgart
Pfaffenwaldring 31, P.O.Box 801140, D-70550 Stuttgart, Germany
e-mail: mattes@ike.uni-stuttgart.de

July 2005

IAEA NUCLEAR DATA SECTION, WAGRAMER STRASSE 5, A-1400 VIENNA

INDC documents may be downloaded in electronic form from http://www-nds.iaea.org/indc_sel.html or sent as an e-mail attachment. Requests for hardcopy or e-mail transmittal should be directed to services@iaea.org or to:

Nuclear Data Section
International Atomic Energy Agency
PO Box 100
Wagramer Strasse 5
A-1400 Vienna
Austria

Produced by the IAEA in Austria
July 2005

Status of Thermal Neutron Scattering Data for Graphite

M. Mattes and J. Keinert

Institute for Nuclear Technology and Energy Systems (IKE) – University of Stuttgart
Pfaffenwaldring 31, P.O.Box 801140, D-70550 Stuttgart, Germany
e-mail: mattes@ike.uni-stuttgart.de

Abstract

At thermal neutron energies, the binding of the scattering nucleus in a solid, liquid, or gas affects the cross sections and the angular and energy distributions of the scattered neutrons. These effects are described in the thermal sub-library of evaluated files in File 7 of the ENDF-6 format.

A re-evaluation of thermal neutron scattering data for carbon bound in graphite has been performed to investigate the impact of models (e.g., generalised frequency distributions) based on different experimental and theoretical data for the generation of scattering law data files $S(\alpha, \beta, T)$ and coherent elastic scattering data.

Two phonon frequency distributions of graphite published in 2002 and 2004 were considered and the results compared with those based on the phonon spectra from Koppel *et al.* (published in 1968), on which the evaluations of ENDF/B-VI and JEFF-3.1 are based. The new frequency distributions were partly derived from *ab initio* simulations.

Detailed comparisons with measurements of differential and integral neutron cross sections and other relevant data are reported.

In addition, thermal MCNP data sets for use in the continuous Monte Carlo codes MCNP and MCNPX were generated from these evaluations for different temperatures. Calculated neutron spectra were found to be in good agreement with the measurements.

Thanks to Dr. Andrej Trkov at IAEA-NDS for the initiation of the work on re-evaluation the thermal neutron scattering data for moderator materials and his continuous interest and support.

This work was partly supported by the IAEA contractual service agreement, contract No. BC: 5380 170 1010 D1000341 EUR 200441839

July 2005

TABLE OF CONTENTS

1.	Introduction	7
2.	History and Status of Thermal Neutron Scattering Data for Graphite	7
3.	Models for the Lattice Dynamics of Graphite	8
4.	Scattering Law Data $S(\alpha, \beta, T)$ for Graphite	11
4.1.	Input to LEAPR.....	11
5.	Validation of the Scattering Law Data Files in ENDF-6 Format	13
5.1.	Scattering Law $S(\alpha, \beta, T)$ for graphite at room temperature	13
5.2.	Scattering Law $S(\alpha, \beta)$ for Graphite at 533 K	16
6.	Validation of the Thermal Neutron Scattering Data for Graphite	17
6.1.	Double Differential Neutron Scattering Cross Sections	17
6.2.	Neutron Cross Sections for Graphite	18
6.2.1.	Inelastic and Elastic Scattering Cross Sections	18
6.2.2.	Total neutron cross section	20
6.3.	Neutron Flux Density Spectra in Graphite	21
6.4.	Recommended Evaluated Data File for Graphite in JEFF-3.1	23
7.	Conclusions	24
	References	25
	Appendix	27
	a) Input to LEAPR for Graphite (GA phonon spectrum)	27
	b) MCNP Data Sets for Graphite	30

List of Figures

3.1	Phonon frequency distributions of polycrystalline graphite	9
3.2	Specific heat for polycrystalline graphite	10
5.1	Scattering law $S(\alpha,\beta)$ for graphite for an energy transfer of 51.7 meV ($\beta=2$)	13
5.2	Scattering law $S(\alpha,\beta)$ for graphite for an energy transfer of 103.4 meV ($\beta=4$)	13
5.3	Scattering law $S(\alpha,\beta)$ for graphite for an energy transfer of 155.1 meV ($\beta=6$)	14
5.4	Scattering law $S(\alpha,\beta)$ for graphite for an energy transfer of 206.8 meV ($\beta=8$)	14
5.5	Scattering law $S(\alpha,\beta)$ for graphite for an energy transfer of 258.5 meV ($\beta=10$)	15
5.6	Scattering law $S(\alpha,\beta)$ for graphite for an energy transfer of 310.2 meV ($\beta=12$)	15
5.7	Scattering law $S(\alpha,\beta)$ for graphite for an energy transfer of 41.3 meV ($\beta=0.9$) at $T=533$ K	16
6.1	Double differential neutron cross section for graphite at room temperature for an initial neutron energy E of 325 meV and for a scattering angle of 120°	17
6.2	Inelastic and coherent elastic neutron scattering cross sections at 293.6 K based on three different phonon frequency distributions	18
6.3	Inelastic neutron scattering cross section for graphite at several temperatures	19
6.4	Coherent elastic neutron scattering cross section for graphite at several temperatures. 19	
6.5	Total neutron cross section for graphite around room temperature	20
6.6	Neutron flux density spectrum of graphite for 274 K and 600 K	21
6.7	Experimental set up for GA-C-5A and 5F taken from the <i>spectrum book</i> [29]	21
6.8	Comparison of calculated neutron spectra in graphite with measurements at 175 °C taken from EACRP-L-62, a compilation of neutron spectra [30]	22
6.9	Neutron spectra in graphite at 325 °C, comparison of MCNPX calculations with the measurement for UK-H-15 taken from EACRP-L-62	22
6.10	Total neutron cross section at room temperature calculated from the existing evaluations in JEFF-3.1 and ENDF/B-VI	23
App.1	Total neutron cross section for graphite as a function of temperature, data are based on the GA frequency distribution	31

List of Tables

3.1	Parameters calculated from $\rho(\omega)$ of graphite at RT	10
4.1	Grid for α and β used in the different evaluations for graphite	11
4.2	Effective scattering temperatures T_{eff} and Debye-Waller integrals $\gamma(0)$ for graphite ...	12
App.1	MCNP Data Sets in the <i>SAB-IKE-2005</i> Library	30

1. Introduction

The scattering of thermal neutrons in graphite is of importance, especially for the Very High Temperature Reactor (VHTR) as a candidate of innovative Generation IV thermal reactor systems. Solid reactor grade graphite as used for HTRs is polycrystalline with a hexagonal lattice structure.

At thermal neutron energies, the binding of the scattering nucleus in a solid moderator material affects the neutron cross sections and the energy and angular distribution of secondary neutrons as the neutron can give up energy to excitations in the material, or it can gain energy. In the evaluated nuclear data files (ENDF/B-VI and JEFF-3.1) these effects are described in the thermal sub-library using File 7 in the ENDF-6 format [1].

For graphite, thermal neutron scattering consists of two parts:

- Inelastic in incoherent approximation represented by $S(\alpha,\beta,T)$, and
- coherent elastic scattering with distinct Bragg edges.

A detailed description of the theory of thermal neutron scattering in matter within the ENDF formalism can be found in [2] and will not be repeated in this document.

2. History and Status of Thermal Neutron Scattering Data for Graphite

- The majority of the work on thermal neutron scattering was performed in the 1950s and 1960s. Subsequently (1970s), data libraries were generated mainly using the GASKET methodology, which was developed at General Atomic (GA) [3, 4]. ENDF files for graphite have been calculated with the “scattering law module” LEAPR [5] of the nuclear data processing system NJOY [6] with the original GA physics model. These data are part of the ENDF/B-VI libraries.
- In JEF-2.2 the scattering law data are carried over from JEF-1 (1984) [7]. The GA model was used in the generation of $S(\alpha,\beta,T)$ for graphite using GASKET-2.
- At PHYSOR 2002 Difilippo [8] presented a phonon frequency distribution for graphite based on earlier work of Nicklow et al [9].
- At PHYSOR 2004 IKE [10] presented a review of the currently used thermal scattering law data $S(\alpha,\beta,T)$ for graphite including the frequency distribution based on *ab initio* methods given by Hawari et al. [11].
- In 2005 the IKE re-evaluation for graphite was accepted for JEFF-3.1 [12]. These $S(\alpha,\beta,T)$ data are based on the GA frequency distribution $\rho(\omega)$ and are calculated by LEAPR with more details in the α and β grids, strictly correlated to the structure of $\rho(\omega)$ and extended to small values for α .

The processing of the generated $S(\alpha,\beta,T)$ was done with NJOY. Comparison with measurements for differential and integral thermal neutron cross sections as well as neutron spectra are given in the following sections.

Experimental data for the verification of generated thermal neutron scattering data are very scarce. Measurements were mainly done in the 1960s, especially at GA in USA, in UK and in Germany at FZK.

3. Models for the Lattice Dynamics of Graphite

An isotropic frequency distribution $\rho(\omega)$ of graphite is necessary as part of the input for the generation of $S(\alpha,\beta,T)$ with LEAPR.

Reactor grade graphite is polycrystalline with a hexagonal lattice structure with four atoms per unit cell, the lattice constants have values $a=b=2.45$ Å, and $c=6.68$ Å. Strong covalent bonding exists between the hexagonal basal planes, while the intra-planar bonding (i.e., between the carbon layers) is of weak van der Waals type. The planes are stacked in an “abab” sequence.

From the lattice dynamics the dispersion relations for graphite can be derived. The frequency distribution $\rho(\omega)$ is then computed with the root sampling method. Three physics models of the central force dynamical studies are published and referred further to:

- **GA model**

The isotropic frequency distribution $\rho(\omega)$ was derived from a general tensor force dynamical model of the unit cells by Yoshimori, Kitano [13] and later improved by Young, Koppel [14]. This was done by the bond-bending and bond-stretching model in adjusting the used force constants to known compressibility and specific heat data. Due to the anisotropy this results in phonon spectra for perpendicular and parallel vibrations of the graphite lattice. Therefore, Young and Koppel have averaged the two parts in Gaussian approximation taking $2/3$ of the parallel and $1/3$ of the perpendicular part. This isotropic distribution was compiled by GA in the so-called *kernel book* [3] and the scattering law data in JEFF-3.1 [12] and ENDF/B-VI [5] are based on this model.

- **ORNL model**

Alternatively, a general tensor force model was examined by Nicklow et al. [9] calling it axially symmetric model and considering C-atoms up to the fourth-nearest neighbours. This model results in an isotropic averaged phonon spectrum of the graphite crystal and was used by Difilippo et al. [8].

- **NCSU model**

Recently Hawari et al. [11] published a new frequency distribution $\rho(\omega)$ of polycrystalline graphite based on the central force dynamical theory with *ab initio* 144 atoms of the hexagonal graphite lattice.

The frequency distribution $\rho(\omega)$ can also be derived from measured double differential neutron scattering cross sections. As $\alpha \rightarrow 0$ the incoherent Scattering Law $S(\alpha,\beta,T)/\alpha$ is correlated to $\rho(\omega)$ in the one phonon excitation formula. In the past many measured $S(\alpha,\beta,T)$ data were used to derive phonon spectra for graphite, i.e., by Egelstaff [15], Whittemore [16], Carvalho [17], Page, Haywood [18] or Butland [19]. However, these phonon spectra often contain multi-phonon contributions of excitations at lower energies which can not be corrected. Therefore only approximate frequency distributions can be derived.

In the following only comparisons for the three theoretical models are presented.

The frequency distributions $\rho(\omega)$ for graphite can be seen in Figure 3.1. Due to the complicated derivation from the dispersion relations (root sampling methods) all curves show a strong peak structure. Generally $\rho(\omega)$ is normalised to unity.

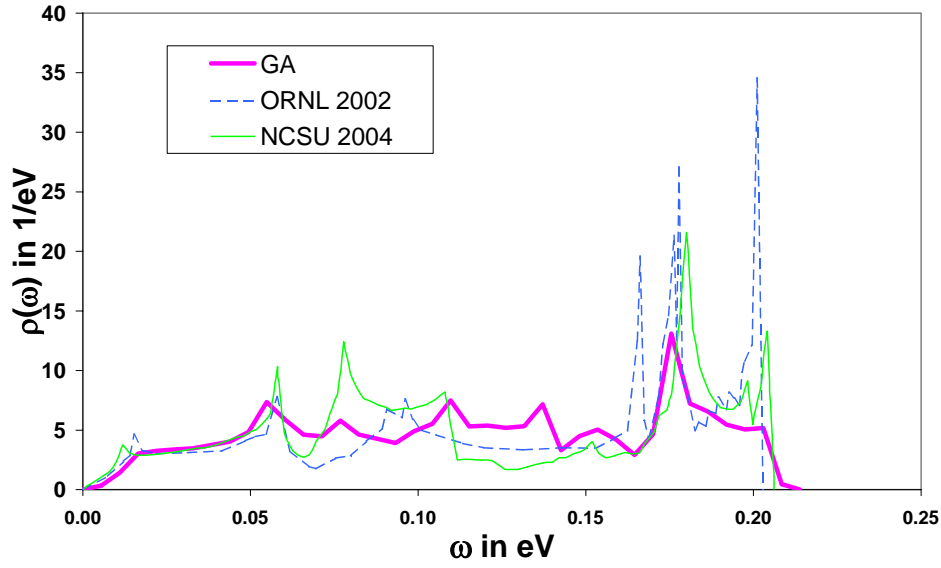


Figure 3.1 Phonon frequency distributions of polycrystalline graphite.

The following parameters are directly correlated to $\rho(\omega)$ such as¹

- the **specific heat relation**

$$\frac{C_V}{3R} = \int_0^{\omega_{\max}} \left(\frac{\omega}{T}\right) \frac{e^{\omega/T}}{(e^{\omega/T} - 1)^2} \rho(\omega) d\omega$$

- the **effective scattering temperature**

$$T_{\text{eff}} = \frac{1}{2} \int_0^{\omega_{\max}} \omega \coth \frac{\omega}{2T} \rho(\omega) d\omega$$

T_{eff} is used for supplementation of the finite α, β -grid of the Scattering Law data file up to infinity according to the short collision time approximation. The average kinetic energy of the system of scattering nuclei is $3/2 T_{\text{eff}}$.

- the **Debye-Waller integral**

$$\gamma(0) = \int_0^{\omega_{\max}} \frac{\rho(\omega)}{\omega} \coth \frac{\omega}{2T} d\omega$$

The Debye-Waller integral is used for calculating the elastic coherent and incoherent neutron scattering cross sections. For coherent scattering the Debye-Waller factor $\exp(-\gamma(0)*\dots)$ describes the height of the cross sections at the Bragg edges and the exponential decrease between them. Also from the Debye-Waller integral the average and maximal atomic displacement can be derived ($\langle u^2 \rangle \sim \gamma(0)$).

- the **average energy transfer**

$$\langle \omega \rangle = \int_0^{\omega_{\max}} \omega \rho(\omega) d\omega$$

The quantity $\langle \omega \rangle$ is a measure of the slowing down quality of the scattering material for thermal neutrons.

¹ \hbar and k are normalised to unity, so that ω and T are in eV

- **the average square of the energy transfer** $\langle \omega^2 \rangle = \int_0^{\omega_{\max}} \omega^2 \rho(\omega) d\omega$

$\langle \omega^2 \rangle$ is correlated to the average $\langle \Delta V \rangle$ of the potential V of the scattering nucleus.

In Table 3.1 these parameters are given for the three phonon frequency spectra of the models from GA, ORNL and NCSU at room temperature RT. In Figure 3.2 the calculated specific heat as a function of temperature is compared with measured values given in [20] and [21].

Table 3.1 Parameters calculated from $\rho(\omega)$ of graphite at RT.

Model	$\langle \omega \rangle / T$	T_{eff} / T	$\langle \omega^2 \rangle / T^2$	$T \bullet \gamma(0)$	$\langle u \rangle$ in Å
GA	4.596	2.43	25.81	0.6586	0.117
ORNL	5.042	2.64	30.67	0.7708	0.126
NCSU	4.649	2.46	26.97	0.9507	0.140

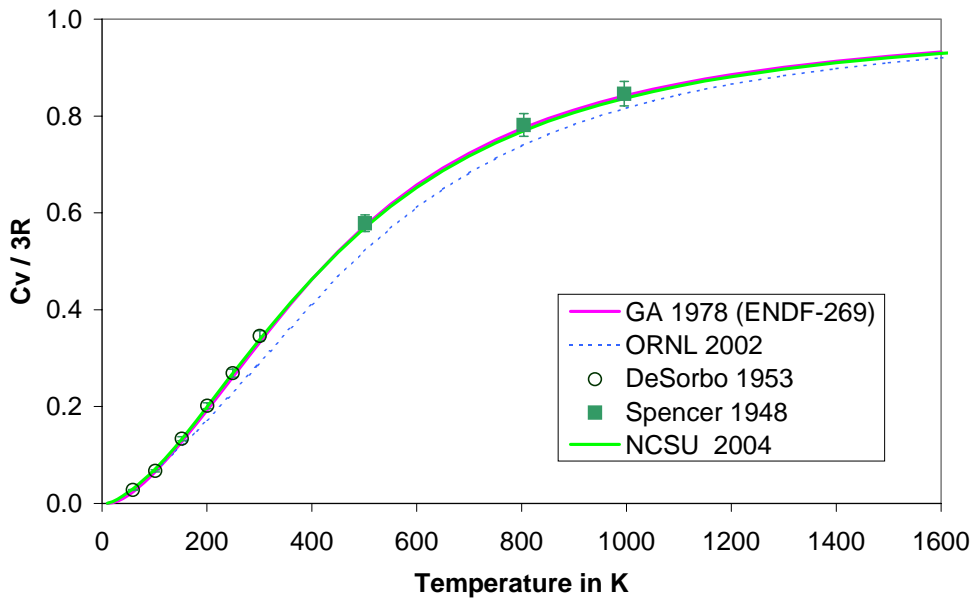


Figure 3.2 Specific heat for polycrystalline graphite.

There is excellent agreement between the GA and NCSU models with the experimental data in the measured temperature range whereas the ORNL model underestimates the specific heat above 200 K. For the GA model this is not surprising because Young and Koppel fitted the force constants in their model to the specific heat.

4. Scattering Law Data $S(\alpha, \beta, T)$ for Graphite

The LEAPR module of NJOY is used to compute the scattering law $S(\alpha, \beta, T)$ and related quantities as T_{eff} and the Debye-Waller integral and the coherent elastic scattering cross section for graphite. The output file is in the ENDF-6 format (MF=7, MT=2 and MT=4) as used by the THERMR module of NJOY. The scattering law $S(\alpha, \beta, T)$ is given in the ENDF format (LAT=1) for each temperature as tables of S versus α for various values of β . Values of S for other values of α and β can be obtained by interpolation.

The dimensionless variables α and β are related to the squared momentum transfer of the scattering nucleus and the energy transfer of the neutron, each divided by kT .

The frequency spectrum $\rho(\omega)$ and an adequate α and β grid at the requested temperatures are necessary as input to LEAPR. For graphite the harmonic approximation is used, that means there is no temperature dependence for $\rho(\omega)$. As graphite has a hexagonal lattice structure the coherent elastic option for graphite is used in LEAPR to generate section MT=2 in MF=7.

For each of the three models $S(\alpha, \beta, T)$ were generated for 11 temperatures between 293.6 K and 3000 K. For the GA model the input for LEAPR is listed in the Appendix.

4.1. Input to LEAPR

LEAPR requires a uniform grid for the continuous frequency distribution $\rho(\omega)$.

For each of the three models GA, ORNL and NCSU an equidistant grid for $\rho(\omega)$ was built and the α and β grid was strongly associated to the maxima and minima of the frequency spectra and its multi-phonon excitations. The α range is extended to small values compared to earlier evaluations. Around the quasi-elastic range of β a fine grid is used. Details of the chosen α, β grids and $E_{\text{max}} (= \beta_{\text{max}} kT)$ are given in Table 4.1.

Table 4.1 Grid for α and β used in the different evaluations for graphite.

Data set	α	range of α	β	range of β	E_{max} (eV)
GA	126	0.00005 – 24.803	185	0 – 73.504	1.86
ORNL	126		214		
NCSU	114		201		
ENDF/B-VI	72	0.01 - 60	96	0 – 80	2.024

The kinematics of the neutron scattering event with a nucleus restricts the maximum value of α to $4\beta_{\text{max}}/A$ which was considered in the generating of $S(\alpha, \beta, T)$ for the GA, ORNL and NCSU models.

The activation energy of diffusion of carbon atoms in the graphite lattice is 1.69 ± 0.12 eV [22]. The upper limit of this value corresponds closely to the chosen value of E_{max} .

If the required α or β is outside the range of the table in File 7, the differential scattering cross section is computed in THERMR using the short-collision-time approximation (SCTA). The effective temperatures T_{eff} needed are included in the data file.

With this choice for the α and β grid, details of the scattering dynamics are well represented in the differential neutron scattering cross section as is given in Figure 6.1.

The atomic weight ratio and free cross section for carbon were taken from ENDF/B-VI.

LEAPR calculates the effective temperatures for the SCT approximation and the Debye-Waller integrals used to compute the coherent elastic scattering. These parameters are shown in Table 4.2 for the GA, ORNL and NCSU models for several temperatures.

Table 4.2 Effective scattering temperatures T_{eff} and Debye-Waller integrals $\gamma(0)$ for graphite.

Temperature K	GA		ORNL		NCSU	
	T_{eff} K	$\gamma(0)$ eV ⁻¹	T_{eff} K	$\gamma(0)$ eV ⁻¹	T_{eff} K	$\gamma(0)$ eV ⁻¹
293.6	713.72	26.22	775.15	30.48	723.07	37.58
400	755.68	32.91	812.00	38.87	765.42	48.40
500	807.58	39.47	858.68	46.98	817.19	58.84
600	869.22	46.20	915.39	55.25	878.41	69.44
700	938.40	53.04	980.18	63.62	947.05	80.16
800	1013.4	59.96	1051.3	72.06	1021.4	90.96
1000	1175.6	73.95	1207.4	89.09	1182.6	112.7
1200	1348.7	88.07	1376.0	106.3	1354.8	134.6
1600	1713.4	116.5	1734.4	140.8	1718.2	178.5
2000	2091.4	145.1	2108.5	175.4	2095.4	222.6
3000	3061.4	216.9	3073.0	262.4	3064.2	333.09

The differences in the values for the two parameters T_{eff} and $\gamma(0)$ are due to the individual frequency distributions. For T_{eff} the upper frequencies are of importance whereas for the Debye-Waller integral the low lying frequencies are most important.

The GA phonon spectra has - compared to the other ones - less pronounced peaks around 200 meV and therefor T_{eff} is generally smaller.

Differences in the Debye-Waller integrals have an effect on the coherent elastic scattering cross section σ_{coh} by the so called Debye-Waller factor in the formula

$$\sigma_{\text{coh}} = \frac{\sigma_b}{E} \sum_{E_i < E} f_i e^{-4\gamma(0)E_i/A}$$

As the GA model gives the lowest values for $\gamma(0)$, the decrease of σ_{coh} with energy will be smaller.

5. Validation of the Scattering Law Data Files in ENDF-6 Format

5.1. Scattering Law $S(\alpha, \beta, T)$ for graphite at room temperature

Measured scattering law data $S(\alpha, \beta, T)$ [16] for graphite at room temperature are available for a variety of energy transfers. In Figures 5.1 to 5.6 comparisons with the computed $S(\alpha, \beta, T)$ for energy transfers from 51.7 meV up to 310 meV for the three models are given. Figure 5.1 shows the scattering law $S(\alpha)$ for $\beta=2$ which describes an energy transfer of 51.7 meV correlated to the second peak region of the phonon spectra.

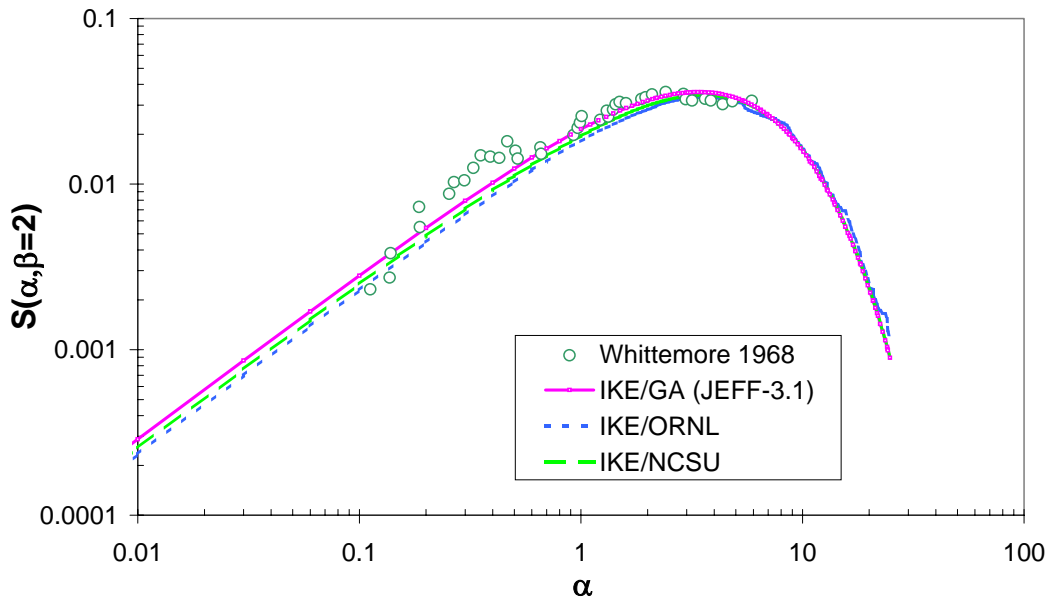


Figure 5.1 Scattering law $S(\alpha, \beta)$ for graphite for an energy transfer of 51.7 meV ($\beta=2$).

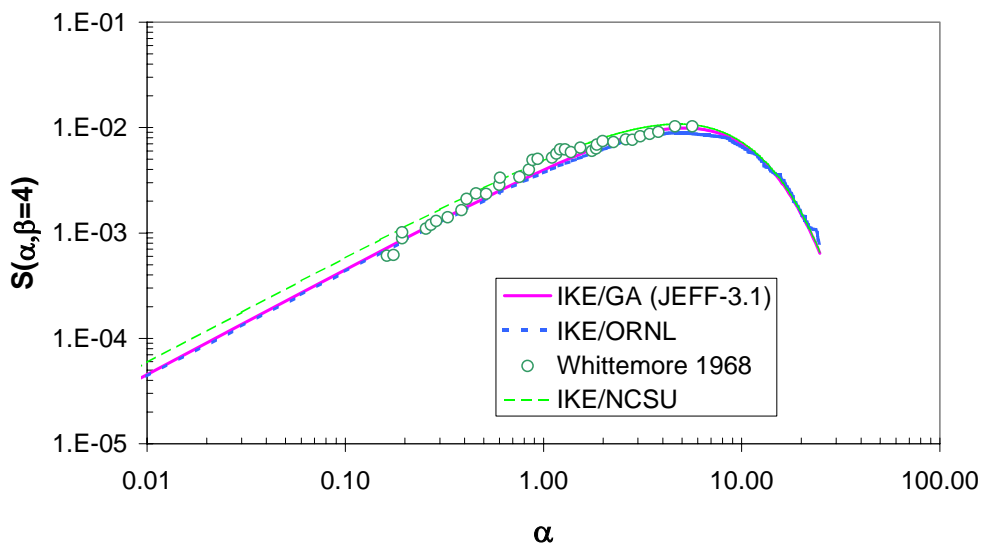


Figure 5.2 Scattering law $S(\alpha, \beta)$ for graphite for an energy transfer of 103.4 meV ($\beta=4$).

The overall agreement with the experimental $S(\alpha, \beta)$ is very good for all of the three models based on different phonon frequency distribution. For an energy transfer of 206.8 meV which corresponds to β equal 8 the GA model fits best the measured values.

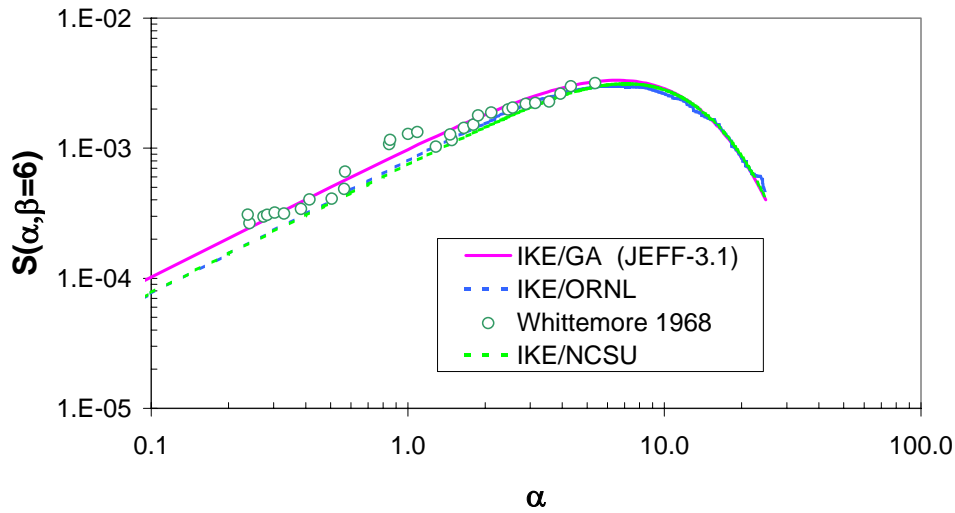


Figure 5.3 Scattering law $S(\alpha, \beta)$ for graphite for an energy transfer of 155.1 meV ($\beta=6$).

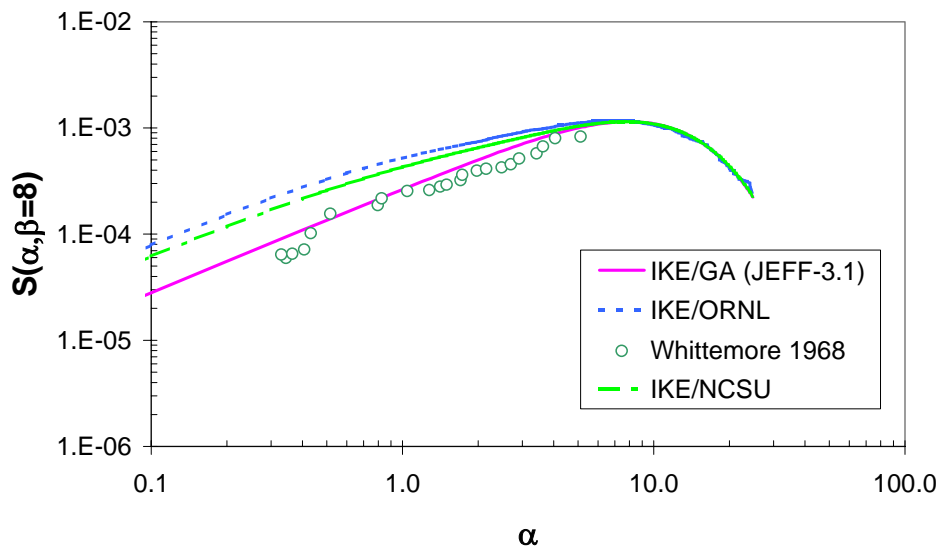


Figure 5.4 Scattering law $S(\alpha, \beta)$ for graphite for an energy transfer of 206.8 meV ($\beta=8$).

For the energy transfer of 206.8 meV, which is correlated to the upper peak structure in $\rho(\omega)$, it seems that for the ORNL and NCSU models these peaks are overestimated.

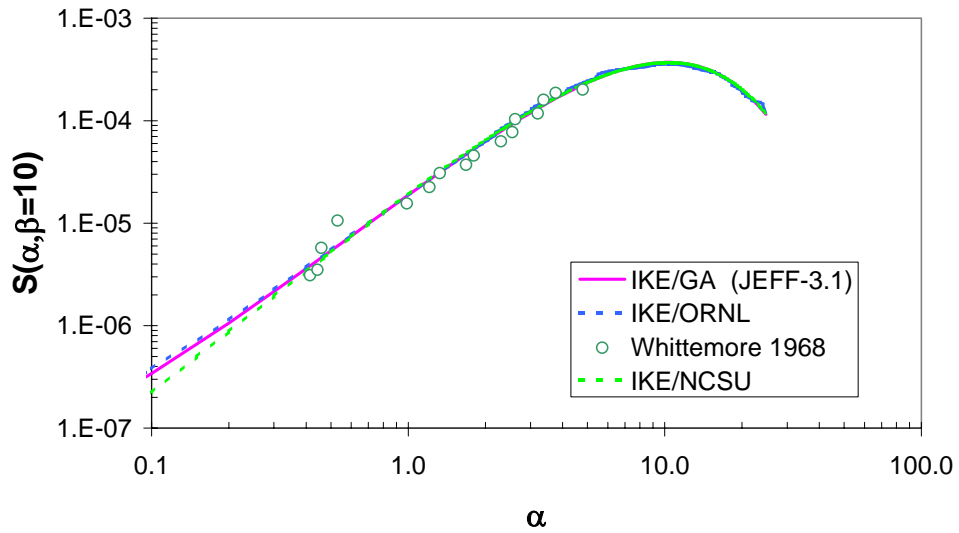


Figure 5.5 Scattering law $S(\alpha,\beta)$ for graphite for an energy transfer of 258.5 meV ($\beta=10$).

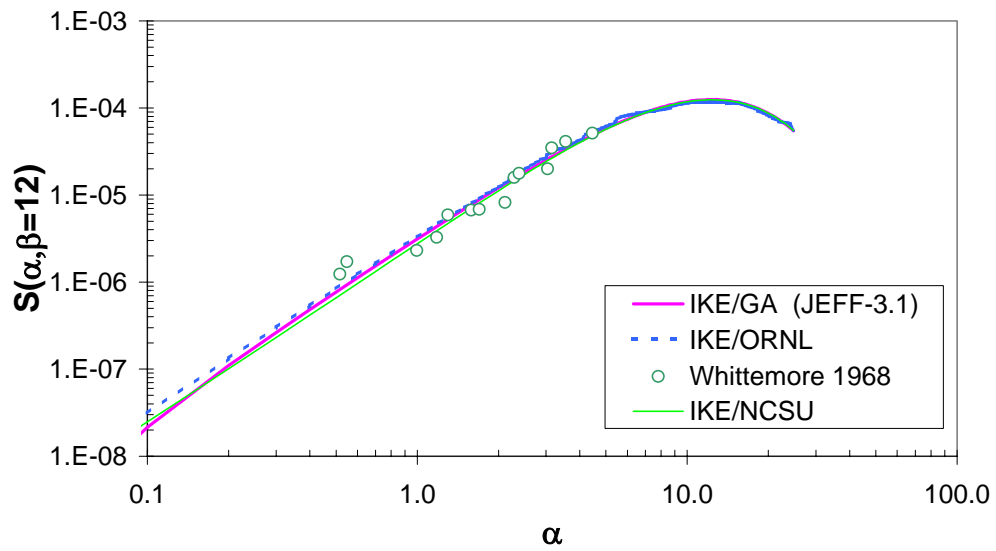


Figure 5.6 Scattering law $S(\alpha,\beta)$ for graphite for an energy transfer of 310.2 meV ($\beta=12$).

5.2. Scattering Law $S(\alpha, \beta)$ for Graphite at 533 K

For 533 K the measured $S(\alpha, \beta)$ from [17] is well represented by the calculated results of the GA, ORNL and NCSU models for this temperature as is shown in Figure 5.7. For this energy transfer the frequency distributions are nearly identical.

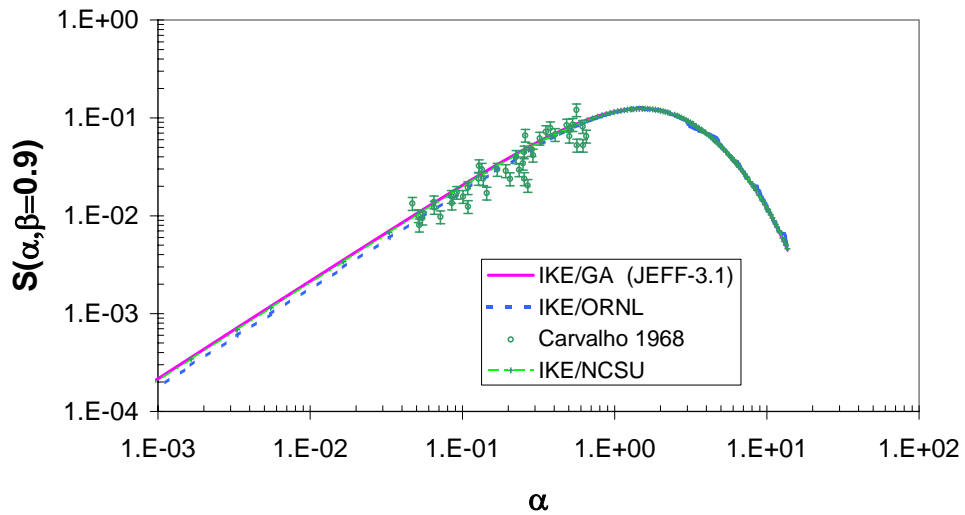


Figure 5.7 Scattering law $S(\alpha, \beta)$ for graphite for an energy transfer of 41.3 meV ($\beta=0.9$) at $T=533$ K.

Unfortunately there are no measurements for values of β which correspond to the peak structure of $\rho(\omega)$.

6. Validation of the Thermal Neutron Scattering Data for Graphite

6.1. Double Differential Neutron Scattering Cross Sections

From the measurements of Whittemore [16] the double differential scattering cross section for graphite with an initial neutron energy of 325 meV and a scattering angle of 120 degree was calculated with the Scattering Law for the three models as given in Figure 6.1.

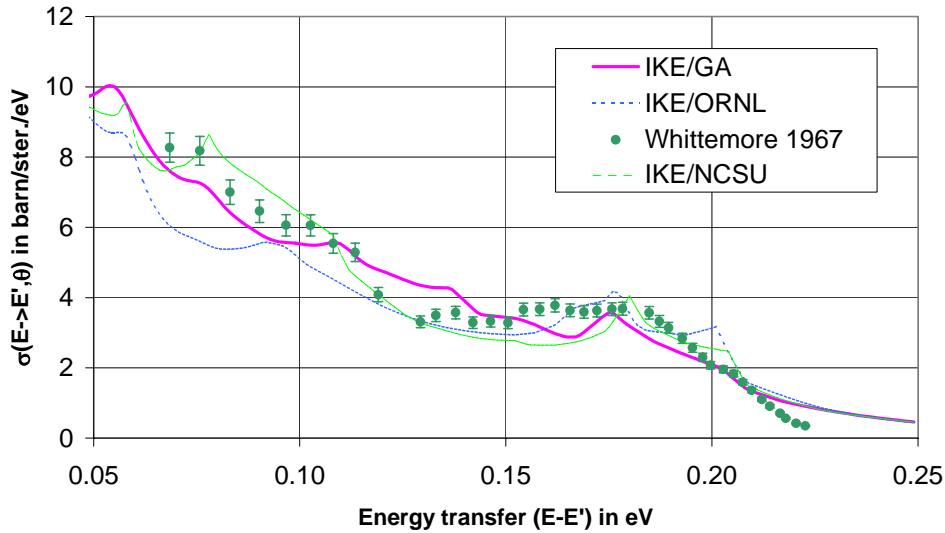


Figure 6.1 Double differential neutron cross section for graphite at room temperature for an initial neutron energy E of 325 meV and for a scattering angle of 120° .

As the abscissa represents the energy transfer of the neutron ($=E_{\text{initial}} - E_{\text{final}}$) the differential cross sections are directly correlated to ω of the different frequency distributions. The different peak structures in $\rho(\omega)$ can be validated with this presentation of the measurement. The peaks around 200 meV which corresponds to the very high peaks in $\rho(\omega)$ for the ORNL and NCSU models are not verified by this experiment.

6.2. Neutron Cross Sections for Graphite

Temperature dependent neutron scattering cross sections for graphite were generated by processing with the module THERMR of NJOY the evaluated thermal neutron files created by LEAPR.

6.2.1. Inelastic and Elastic Scattering Cross Sections

The two parts of the neutron scattering cross section in graphite

- Inelastic scattering as described by the scattering law $S(\alpha, \beta, T)$ in incoherent approximation
- Coherent elastic scattering

are shown in Figure 6.2 for the three evaluations based on the GA, ORNL and NCSU models.

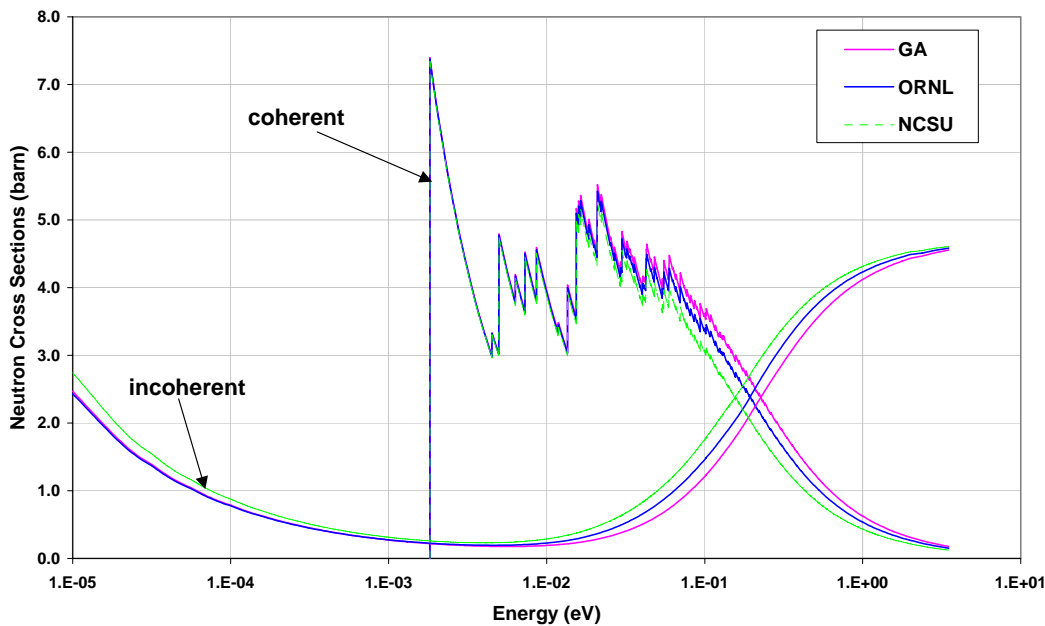


Figure 6.2 Inelastic and coherent elastic neutron scattering cross sections at 293.6 K based on three different phonon frequency distributions.

The coherent elastic part of the thermal neutron scattering cross sections from the three data sets differ due to the different Debye-Waller integrals as given in Table 3.1 as a result of different phonon spectra. This is valid also for the inelastic neutron cross sections of the three evaluations. It is clearly seen that for the total neutron scattering cross section (sum of the parts) there will be compensation effects in the important energy range for nuclear applications (see Figure 6.5).

The inelastic neutron scattering cross sections (incoherent approximation) for different temperatures are shown in Figure 6.3. For all models the curves differ significantly. The same holds for the coherent elastic scattering cross sections given in Figure 6.4.

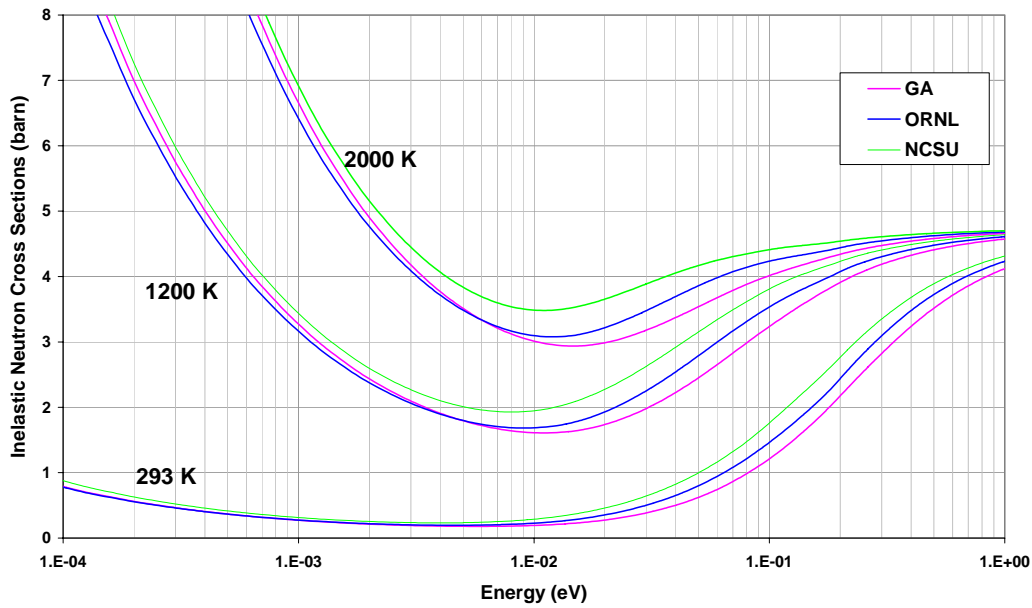


Figure 6.3 Inelastic neutron scattering cross section for graphite at several temperatures.

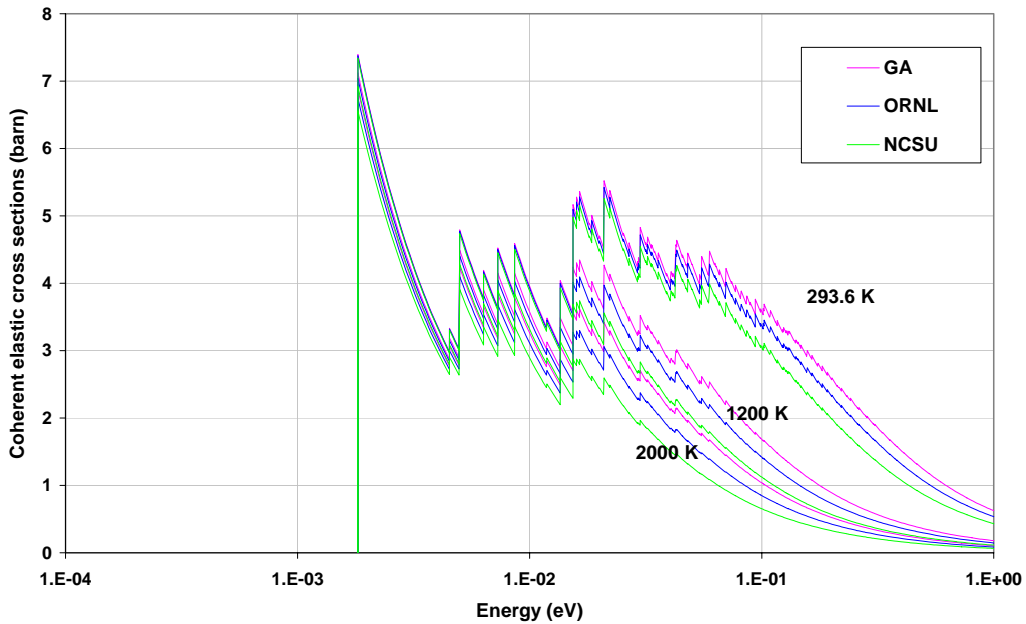


Figure 6.4 Coherent elastic neutron scattering cross section for graphite at several temperatures.

6.2.2. Total neutron cross section

The total neutron cross section for graphite as a function of energy is shown in Figure 6.5 for room temperature. There is good agreement between the three evaluated data sets. However the partial scattering cross sections (inelastic and coherent elastic) differ as shown in Figure 6.2.

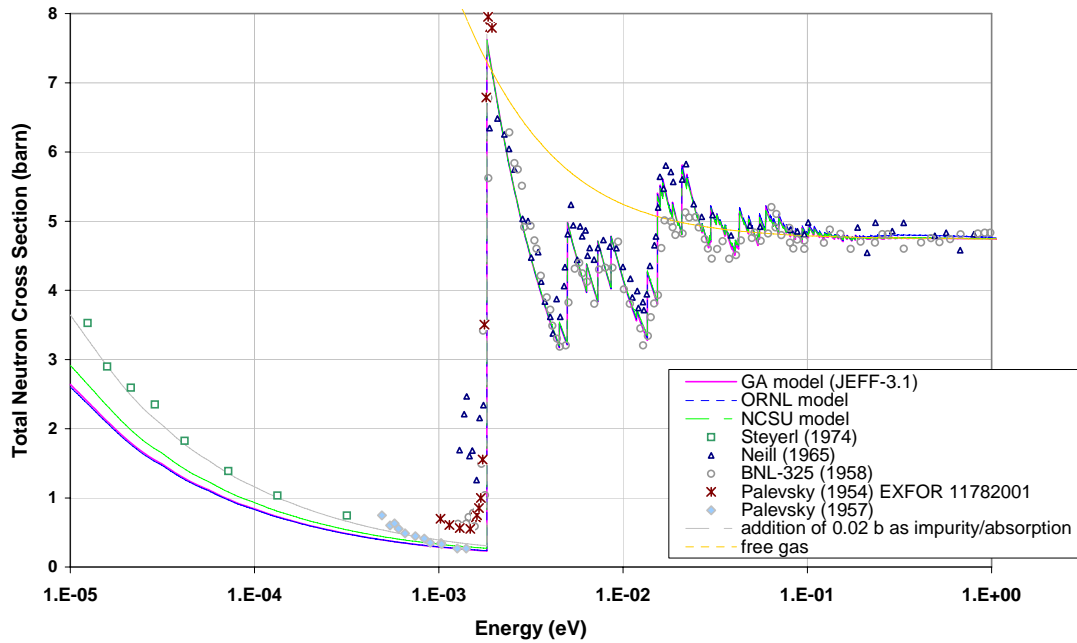


Figure 6.5 Total neutron cross section for graphite around room temperature.

As can be seen in Figure 6.5 the total neutron cross section is underestimated at low energies compared to experimental results. However an additional small contribution of a pseudo absorption ($1/v$ -behavior assumed) representing a small impurity in graphite shows good agreement. In the measurements [23-27] the specification of the graphite and impurities are not given. The experimental data of Palevsky (1957) are taken from Kothari, Singwi [26].

6.3 Neutron Flux Density Spectra in Graphite

MCNP data sets in ACE format based on the three physics models were generated with NJOY using the modules THERMR and ACER for 16 angles and 64 equally energy bins for the secondary energies. For the verification of the data neutron flux density spectra in graphite were calculated [28] with MCNP-4C3 and MCNPX Monte Carlo codes and compared with experiments. As an example Figure 6.6 shows the results for graphite at 274 K and 600 K for the three data sets based on the GA model as well as the ORNL and NCSU models. The measured values are taken from [29] for the two configurations GA-C-5A and GA-C-5F as shown in Figure 6.7.

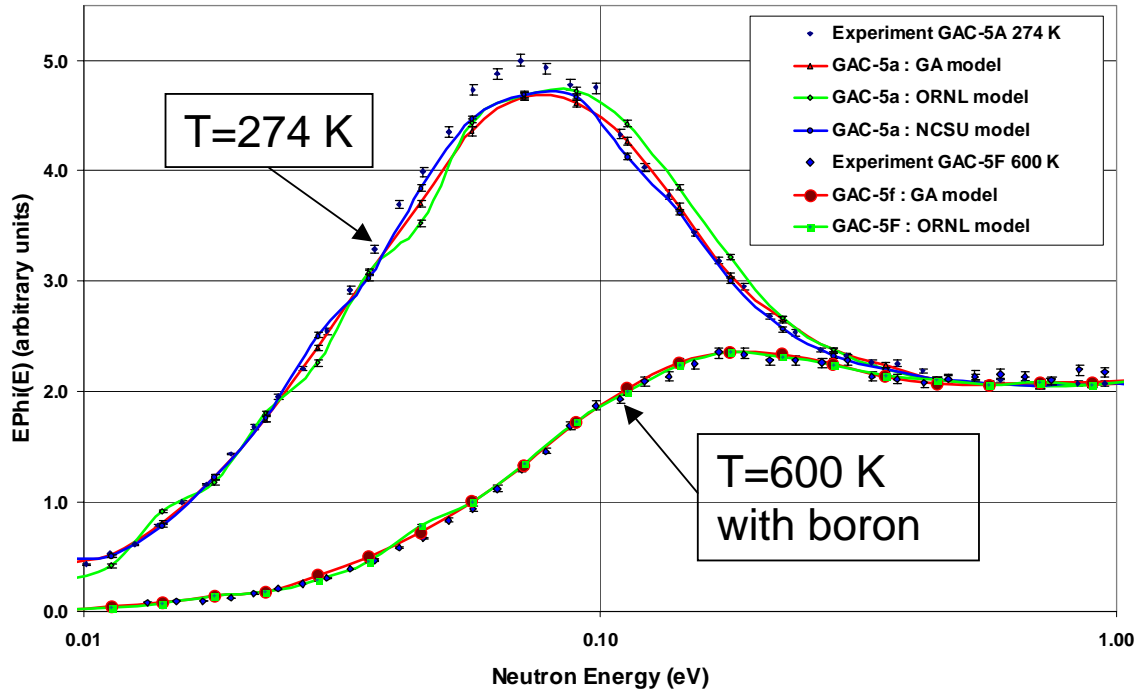


Figure 6.6 Neutron flux density spectrum of graphite for 274 K and 600 K.

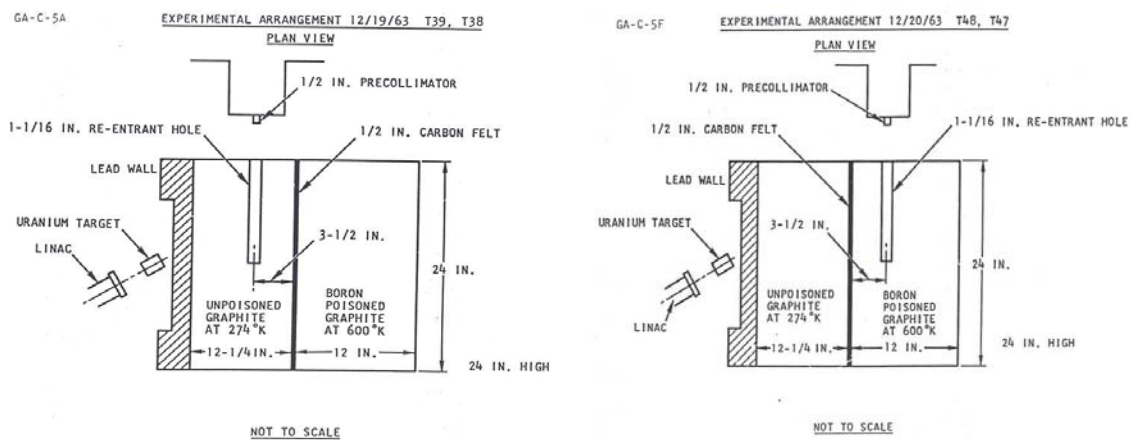


Figure 6.7 Experimental set-up for GA-C-5A and 5F taken from the *spectrum book* [29].

For the higher temperature the agreement is excellent, whereas at 274 K for the pure graphite assembly the maximum of the spectrum is underestimated by all data sets.

A very good agreement between measured and calculated neutron spectra can be seen for the temperatures of 35 °C, 175 °C and 325 °C from the experiments UK-H-7 and UK-H-15 done at Harwell and compiled in [30].

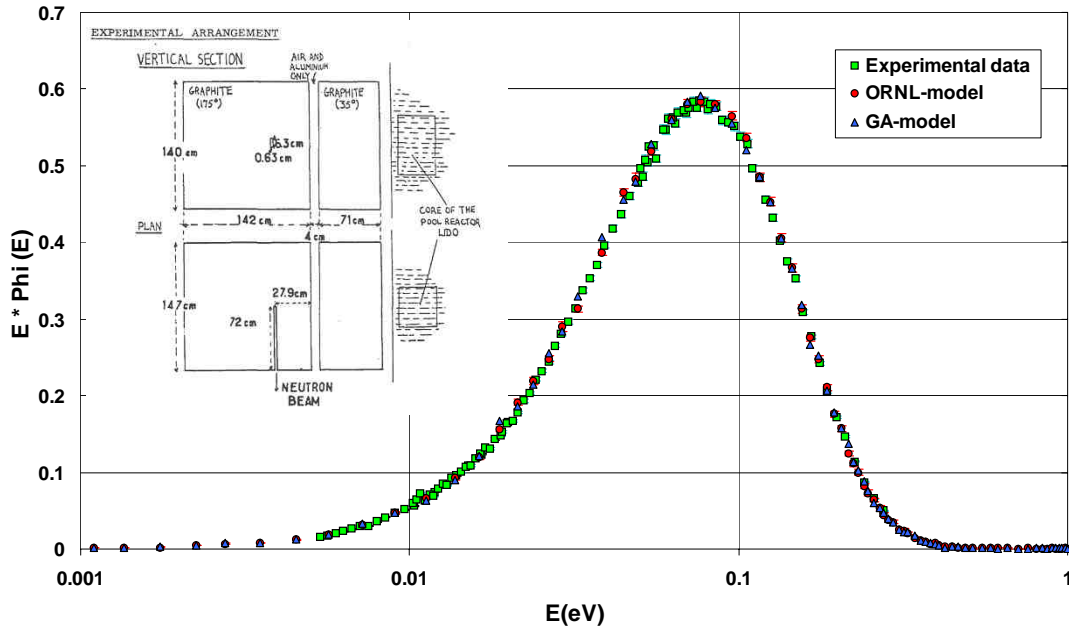


Figure 6.8 Comparison of calculated neutron spectra in graphite with measurements at 175 °C taken from EACRP-L-62, a compilation of neutron spectra [30].

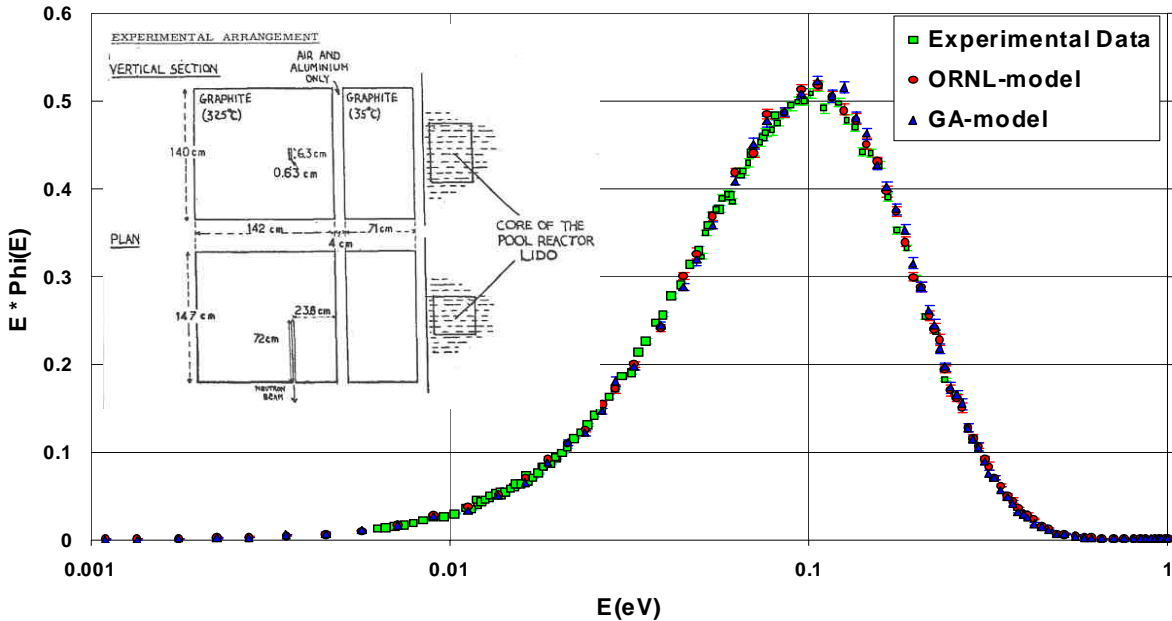


Figure 6.9 Neutron spectra in graphite at 325 °C, comparison of MCNPX calculations with the measurement for UK-H-15 taken from EACRP-L-62.

6.4. Recommended Evaluated Data File for Graphite in JEFF-3.1

The overall agreement of the evaluation for graphite based on the GA model with measured double-differential neutron cross sections and measured scattering laws as well as the correct prediction of the total neutron cross section results in the recommendation to use this evaluation for JEFF-3.1.

Furthermore a long experience in the field of nuclear applications using the GA phonon spectra for graphite support this decision. For the operating temperatures of HTRs unfortunately there is a lack of available measurements to compare with.

Results of studies as presented in [10] or at the Workshop on Nuclear Data Needs for Generation IV Nuclear Energy Systems at Antwerp (April 2005) [28] [31] have shown that the three different phonon spectra (GA,ORNL, NCSU) did not give any remarkable differences in intensive and detailed MCNP(X) calculations for k_{eff} and other related quantities.

For measured differential neutron cross section the NCSU model yields comparable results as the GA model whereas the ORNL model shows discrepancies for the specific heat. However for energy transfers correlated to the peaks in the high energy part in the phonon spectra there are shortcomings for both the ORNL and NCSU models.

The JEFF-3.1 thermal neutron scattering data are based on the GA phonon spectra like the ENDF/B-VI evaluation, but the generation of the $S(\alpha,\beta,T)$ was done on different α,β grids. The effect on the total neutron cross sections at room temperature is very small as shown in Figure 6.10.

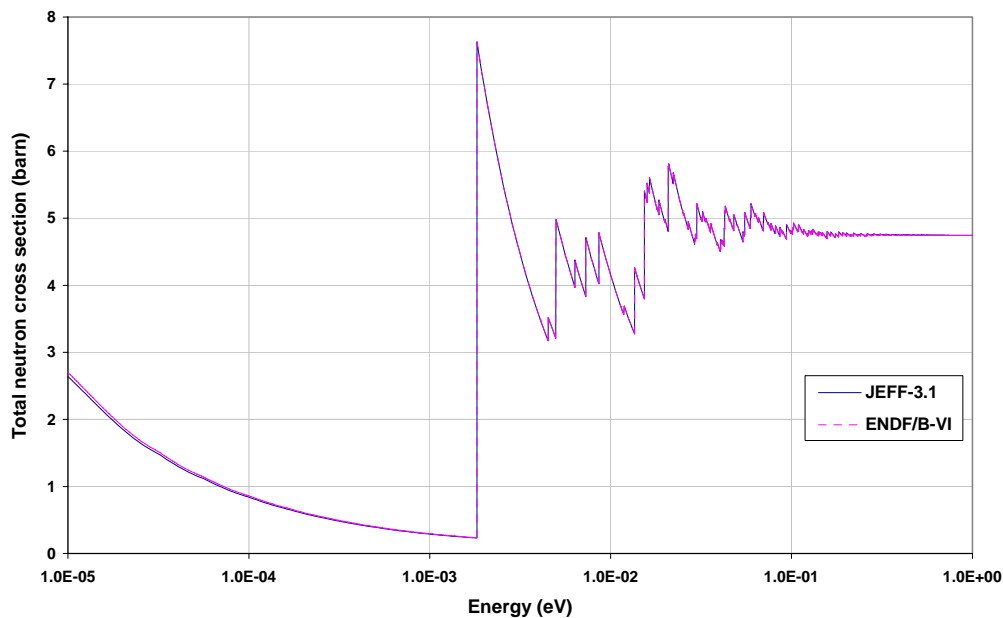


Figure 6.10 Total neutron cross section at room temperature calculated from the existing evaluations in JEFF-3.1 and ENDF/B-VI.

7. Conclusions

The adequacy of thermal neutron scattering data for graphite was re-considered in view of three phonon spectra from GA, ORNL and NCSU, currently available. The following conclusions can be drawn:

- There were hardly any new experimental measurements performed since the time the thermal scattering methods were developed.
- Existing models are able to describe available experimental data very well. The GA model represents better the specific heat relation compared to ORNL model, whereas the NCSU model is comparable to the GA model. Important is a suitable α, β -grid oriented at the frequency distributions for the representation of the scattering law data.
- Significant differences between the partial thermal scattering cross sections for the different phonon spectra were observed. However the total neutron cross sections for the three frequency spectra agree very well and the three models did not give any remarkable differences in the intensive and detailed MCNP calculations of k_{eff} and k_{∞} . Neutron spectra at different temperatures are well reproduced.
- New thermal neutron scattering libraries are available from the IAEA-NDS web site.
- The GA model was selected for the final recommended thermal scattering law library.

REFERENCES

- [1] MCLANE, V., Ed., "ENDF-102: Data Formats and Procedures for the Evaluated Nuclear Data File ENDF-6," Brookhaven National Laboratory report BNL-NCS-44945 -01/04-Rev. (April 2001), <http://www.nndc.bnl.gov/nndcscr/documents/endl/endl102/>.
- [2] MATTES, M., KEINERT, J.: "Thermal Neutron Scattering Data for the Moderator Materials H₂O, D₂O and ZrH_x in ENDF-6 Format and as ACE Library for MCNP(X) Codes", INDC(NDS)-0470 (April 2005), report and data (both formats) are available from <http://www-nds.iaea.org/indlts/>.
- [3] KOPPEL, J. U., HOUSTON, D. H., "Reference Manual for ENDF Thermal Neutron Scattering Data," General Atomics report GA-8774 revised and reissued as ENDF-269 by the National Nuclear Data Center at the BNL (July 1978).
- [4] KOPPEL, J.U., TRIPLETT, J.R., NALIBOFF, Y.D., "GASKET: A Unified Code for Thermal Neutron Scattering," General Atomics report GA-7417 (Rev.) (March 1967).
- [5] MACFARLANE, R.E., "New Thermal Neutron Scattering Files for ENDF/B-VI, Release 2", LA-12639-MS (August 1994).
- [6] MACFARLANE, R. E., MUIR, D.W., "The NJOY Nuclear Data Processing System", LA-12740-M (1994).
- [7] KEINERT, J., MATTES, M., "JEF-1 Scattering Law Data", IKE 6-147 / JEF Report 2 / JEF/DOC 41.2 (1984).
- [8] DIFILIPPO, F.C., RENIER, J.P., HAWARI, A.I., "Benchmarks for the Scattering Kernel of Graphite," Proceedings of the PHYSOR 2002: International Conference on the New Frontiers of Nuclear Technology, Seoul, South Korea, October 7-10 (2002).
- [9] NICKLOW, R., WAKABAYASHI, N., SMITH, H. G., "Lattice Dynamics of Pyrolytic Graphite," *Phys. Rev. B* 5, 4951 (1972).
- [10] BERNNAT, W., KEINERT, J., MATTES, M., "Scattering Law Data for Graphite in Gas Cooled High Temperature Reactors", PHYSOR 2004, Chicago, Illinois, April 25-29 (2004).
- [11] HAWARI, A.I., AL-QASIR, I., GILLETTE, V.H., WEHRING, B.W., ZHOU, T. "Ab Initio Generation of Thermal Neutron Scattering Cross Sections", PHYSOR 2004, Chicago, Illinois, April 25-29 (2004).
- [12] JEFF-3.1, Contents of the thermal scattering law data files <http://www.nea.fr/html/dbdata/JEFF/JEFF31/index-JEFF-TS.html>.
- [13] YOSHIMORI, A., KITANO, Y., "Theory of the Lattice Vibration of Graphite", *J. Phys. Soc. Japan* 11, 352 (1956).
- [14] YOUNG, J.A., KOPPEL, J.U., "Phonon Spectrum of Graphite", *J. Chem. Phys.* **42**, 357 (1965).
- [15] EGELSTAFF, P.A., "Compilation of Early Scattering Law Data", AERE-R-3931 (1962).
- [16] WHITTEMORE, W.L., "Neutron Scattering by Reactor-Grade Graphite", *Nucl. Sci. Eng.* **33**, 31 (1968).
- [17] CARVALHO, F., "Inelastic Scattering of Thermal Neutrons in Graphite", *Nucl. Sci. Eng.* **34**, 224 (1968).
- [18] PAGE, D.I., HAYWOOD, B.C., "The HARWELL Scattering Law Programme: Frequency Distributions of Moderators", AERE-R 5778 (1968).
- [19] BUTLAND, A.T.D., "The generation of improved thermal neutron scattering models for graphite", AEEW-R-882 (1973).
- [20] DE SORBO, W., TYLER, W.W., "The specific heat of graphite from 13 to 300K", *J. Chem. Phys.* **21**, 1660 (1953).

- [21] SPENCER, H.M., "Empirical heat capacity equation of gases and graphite", *J. Ind. Eng. Chem.* **40**, 2152 (1948).
- [22] KANTER, M.A., "Diffusion in Carbon Atoms in Natural Graphite Crystals", *Phys. Rev.* **107**, 655 (1957).
- [23] STEYERL, A., TRÜSTEDT, W.D., "Experiments with a Neutron Bottle," *Z. Physik* **267**, 379 (1974).
- [24] NEILL, J.M., et al., "Integral Neutron Thermalization," GA-6753 (1965).
- [25] HUGHES, D.J., SCHWARTZ, R.B., "Neutron Cross Sections" BNL-325 (1958).
- [26] KOTHARI, L.S., SINGWI, K.S., "Thermal Inelastic Scattering of Cold Neutrons in Polycrystalline Graphite", *Phys. Rev.* **106**, 230 (1957).
- [27] PALEVSKY, H., HUGHES, D.J., ZIMMERMAN, R.L., " Inelastic Scattering of Cold Neutrons by the Lattice Vibration of Crystalline Solids", *J. Phys. Rev.* **99**, 11 B11 (1955) > EXFOR 11782001.
- [28] BERNNAT, W., private communication, 2004 and Workshop on Nuclear Data Needs for Generation IV Nuclear Energy Systems, Antwerp 5-7 April 2005.
- [29] "Experimental and Theoretical Neutron Spectra"; compiled by J.C. Young, and D. Huffmann, GA-5319 (1964).
- [30] "Neutron Spectra", EACRP-L-62 (1966).
- [31] YOUNG-SIK Cho, "Comparative Study on Different Phonon Frequency Spectra of Graphite in GCR", Workshop on Nuclear Data Needs for Generation IV Nuclear Energy Systems, Antwerp 5-7 April 2005.

APPENDIX

a) Input to LEAPR for Graphite (GA phonon spectrum)

For computing the thermal neutron scattering data for graphite using the GA model for the inelastic part ($S(\alpha, \beta)$) and the coherent elastic scattering the input to the module LEAPR of NJOY-90.99 are listed in the following:

```

leapr
40
'GRAPHITE, GA model as used at IKE (2004) ' /
11 1/
31 131./
11.898 4.73924 1 1/   xs from ENDF/B-VI
0/
126 185 1/   new alpha beta grid for INDL/TSL and IKE-JEFF-3.1
.00005 .0001 .0005 .0010 .0030 .0060
.01 .03 .06
.1000
.2000 .3000 .4000 .5000 .6000 .7000 .8000
.9000 1.0000 1.1000 1.2000 1.3000 1.4000 1.5000
1.6000 1.7000 1.8000 1.9000 2.0000 2.1000 2.1680
2.2023 2.3070 2.4142 2.5238 2.6360 2.7509 2.8684
2.9886 3.0350 3.1116 3.2375 3.3664 3.4982 3.6331
3.7712 3.9124 4.0570 4.2049 4.3360 4.5112 4.6697
4.8319 4.9979 5.1677 5.3416 5.4200 5.5194 5.7014
5.8877 6.0700 6.2733 6.4728 6.5040 6.6771 6.8860
6.9370 7.0999 7.3187 7.5426 7.7718 8.0210 8.2462
8.4917 8.6720 8.7430 9.0001 9.1050 9.2632 9.5324
9.8080 10.0899 10.3784 10.6736 10.8400 10.9757 11.2848
11.6011 11.9249 12.1400 12.2561 12.5951 12.9419 13.0080
13.2969 13.6601 13.8750 14.0318 14.4121 14.8013 15.1760
15.6071 16.0420 16.2600 16.4510 16.8877 17.3440 17.7918
18.2110 18.2598 18.7386 19.2287 19.7301 20.2432 20.7683
20.8120 21.3056 21.6800 21.8554 22.4180 22.9937 23.5829
24.0630 24.1858 24.2810 24.8027 /
.0000 .0010 .0050 .0100 .0500 .1000 .1500
.2000 .2500 .3000 .3500 .4000 .4500 .5000
.5500 .6000 .6500 .7000 .7500 .8000 .8500
.9000 .9500 1.0000 1.0500 1.1000 1.1500 1.2000
1.2500 1.3000 1.3500 1.4000 1.4500 1.5000 1.5500
1.6000 1.6500 1.7000 1.7500 1.8000 1.8500 1.9000
1.9500 2.0000 2.0500 2.1000 2.1500 2.1679 2.2000
2.2500 2.3000 2.3500 2.4000 2.4500 2.5000 2.5500
2.6000 2.6500 2.7000 2.7500 2.8000 2.8500 2.9000
2.9500 3.0000 3.0351 3.0500 3.1000 3.1500 3.2000
3.2500 3.3000 3.3500 3.4000 3.4500 3.5000 3.5500
3.6000 3.6500 3.7000 3.7500 3.8000 3.8500 3.9000
3.9500 4.0000 4.0500 4.1034 4.1605 4.2215 4.2866
4.3359 4.3562 4.4306 4.5100 4.5949 4.6856 4.7825
4.8860 4.9967 5.1148 5.2411 5.3760 5.4200 5.5201
5.6740 5.8386 6.0143 6.0702 6.2021 6.4027 6.5037
6.6171 6.8461 6.9374 7.0907 7.3521 7.6314 7.9298
8.0211 8.2486 8.5892 8.6716 8.9531 9.1053 9.3419
9.7573 10.2011 10.6753 10.8400 11.1819 11.7231 12.1404
12.3014 12.9192 13.0077 13.5793 13.8748 14.2845 15.0379
15.1755 15.8429 16.0422 16.2600 16.7030 17.3436 17.6219
18.2106 18.6036 19.6525 20.7731 20.8122 21.6795 21.9704
23.2496 24.0633 24.2808 24.6162 26.0764 27.1000 27.6364
27.7496 29.3032 30.3510 31.0839 32.0844 32.9864 34.6870
35.0191 37.1908 39.5111 40.1055 41.9900 44.6385 47.4682
48.1266 50.4914 53.7214 56.1477 57.1724 60.8594 64.1688
64.7986 69.0072 73.5037 /
293.6 /
0.0004388 489 / uniform grid for phonon spectra (GA model), parable
0.
2.213E-03 8.852E-03 1.992E-02 3.541E-02 5.532E-02 7.967E-02
1.084E-01 1.416E-01 1.792E-01 2.213E-01 2.678E-01 3.187E-01
3.883E-01 4.735E-01 5.586E-01 6.438E-01 7.289E-01 8.141E-01
8.992E-01 9.844E-01 1.070E+00 1.155E+00 1.240E+00 1.325E+00
1.410E+00 1.539E+00 1.669E+00 1.798E+00 1.927E+00 2.056E+00
2.186E+00 2.315E+00 2.444E+00 2.573E+00 2.703E+00 2.832E+00
2.961E+00 3.035E+00 3.053E+00 3.071E+00 3.089E+00 3.107E+00
3.125E+00 3.143E+00 3.161E+00 3.179E+00 3.197E+00 3.215E+00
3.233E+00 3.251E+00 3.261E+00 3.271E+00 3.281E+00 3.291E+00
3.301E+00 3.311E+00 3.321E+00 3.331E+00 3.341E+00 3.351E+00

```

3.361E+00 3.371E+00 3.380E+00 3.388E+00 3.396E+00 3.404E+00
3.412E+00 3.420E+00 3.427E+00 3.435E+00 3.443E+00 3.451E+00
3.459E+00 3.466E+00 3.474E+00 3.497E+00 3.519E+00 3.542E+00
3.564E+00 3.586E+00 3.609E+00 3.631E+00 3.654E+00 3.676E+00
3.699E+00 3.721E+00 3.744E+00 3.766E+00 3.789E+00 3.812E+00
3.835E+00 3.858E+00 3.881E+00 3.903E+00 3.926E+00 3.949E+00
3.972E+00 3.995E+00 4.018E+00 4.040E+00 4.104E+00 4.168E+00
4.231E+00 4.295E+00 4.358E+00 4.422E+00 4.486E+00 4.549E+00
4.613E+00 4.676E+00 4.740E+00 4.803E+00 4.935E+00 5.136E+00
5.336E+00 5.536E+00 5.737E+00 5.937E+00 6.138E+00 6.338E+00
6.538E+00 6.739E+00 6.939E+00 7.139E+00 7.340E+00 7.222E+00
7.104E+00 6.986E+00 6.869E+00 6.751E+00 6.633E+00 6.516E+00
6.398E+00 6.280E+00 6.162E+00 6.045E+00 5.927E+00 5.818E+00
5.718E+00 5.619E+00 5.519E+00 5.419E+00 5.319E+00 5.220E+00
5.120E+00 5.020E+00 4.921E+00 4.821E+00 4.721E+00 4.621E+00
4.609E+00 4.597E+00 4.586E+00 4.574E+00 4.562E+00 4.550E+00
4.538E+00 4.526E+00 4.514E+00 4.502E+00 4.490E+00 4.478E+00
4.525E+00 4.630E+00 4.736E+00 4.842E+00 4.947E+00 5.053E+00
5.159E+00 5.264E+00 5.370E+00 5.475E+00 5.581E+00 5.687E+00
5.792E+00 5.699E+00 5.606E+00 5.513E+00 5.419E+00 5.326E+00
5.233E+00 5.140E+00 5.046E+00 4.953E+00 4.860E+00 4.767E+00
4.673E+00 4.613E+00 4.585E+00 4.556E+00 4.528E+00 4.500E+00
4.472E+00 4.444E+00 4.416E+00 4.387E+00 4.359E+00 4.331E+00
4.303E+00 4.275E+00 4.246E+00 4.217E+00 4.187E+00 4.158E+00
4.129E+00 4.100E+00 4.071E+00 4.042E+00 4.013E+00 3.984E+00
3.955E+00 3.926E+00 3.951E+00 4.030E+00 4.109E+00 4.189E+00
4.268E+00 4.347E+00 4.426E+00 4.505E+00 4.585E+00 4.664E+00
4.743E+00 4.822E+00 4.902E+00 4.951E+00 5.001E+00 5.051E+00
5.101E+00 5.151E+00 5.201E+00 5.251E+00 5.301E+00 5.350E+00
5.400E+00 5.450E+00 5.500E+00 5.604E+00 5.761E+00 5.918E+00
6.076E+00 6.233E+00 6.391E+00 6.548E+00 6.706E+00 6.863E+00
7.020E+00 7.178E+00 7.335E+00 7.493E+00 7.317E+00 7.142E+00
6.967E+00 6.792E+00 6.617E+00 6.442E+00 6.267E+00 6.092E+00
5.917E+00 5.741E+00 5.566E+00 5.391E+00 5.307E+00 5.314E+00
5.321E+00 5.328E+00 5.336E+00 5.343E+00 5.350E+00 5.357E+00
5.364E+00 5.371E+00 5.378E+00 5.385E+00 5.392E+00 5.376E+00
5.360E+00 5.344E+00 5.328E+00 5.312E+00 5.296E+00 5.280E+00
5.264E+00 5.247E+00 5.231E+00 5.215E+00 5.199E+00 5.196E+00
5.206E+00 5.216E+00 5.226E+00 5.236E+00 5.246E+00 5.255E+00
5.265E+00 5.275E+00 5.285E+00 5.295E+00 5.305E+00 5.315E+00
5.462E+00 5.609E+00 5.756E+00 5.904E+00 6.051E+00 6.198E+00
6.345E+00 6.493E+00 6.640E+00 6.787E+00 6.934E+00 7.082E+00
7.001E+00 6.694E+00 6.386E+00 6.079E+00 5.771E+00 5.463E+00
5.156E+00 4.848E+00 4.541E+00 4.233E+00 3.925E+00 3.618E+00
3.310E+00 3.405E+00 3.499E+00 3.593E+00 3.688E+00 3.782E+00
3.877E+00 3.971E+00 4.065E+00 4.160E+00 4.254E+00 4.349E+00
4.443E+00 4.512E+00 4.556E+00 4.599E+00 4.643E+00 4.686E+00
4.730E+00 4.773E+00 4.817E+00 4.860E+00 4.904E+00 4.947E+00
4.991E+00 5.034E+00 4.968E+00 4.901E+00 4.834E+00 4.767E+00
4.700E+00 4.633E+00 4.566E+00 4.500E+00 4.433E+00 4.366E+00
4.299E+00 4.232E+00 4.147E+00 4.044E+00 3.942E+00 3.839E+00
3.736E+00 3.633E+00 3.530E+00 3.427E+00 3.324E+00 3.221E+00
3.119E+00 3.016E+00 2.913E+00 3.051E+00 3.189E+00 3.327E+00
3.465E+00 3.604E+00 3.742E+00 3.880E+00 4.018E+00 4.156E+00
4.294E+00 4.433E+00 4.571E+00 4.978E+00 5.655E+00 6.332E+00
7.009E+00 7.686E+00 8.363E+00 9.039E+00 9.716E+00 1.039E+01
1.107E+01 1.175E+01 1.242E+01 1.310E+01 1.263E+01 1.216E+01
1.169E+01 1.122E+01 1.075E+01 1.028E+01 9.815E+00 9.345E+00
8.876E+00 8.406E+00 7.937E+00 7.467E+00 7.205E+00 7.151E+00
7.096E+00 7.042E+00 6.987E+00 6.932E+00 6.878E+00 6.823E+00
6.769E+00 6.714E+00 6.659E+00 6.605E+00 6.550E+00 6.463E+00
6.376E+00 6.288E+00 6.201E+00 6.114E+00 6.026E+00 5.939E+00
5.852E+00 5.764E+00 5.677E+00 5.590E+00 5.502E+00 5.442E+00
5.409E+00 5.377E+00 5.344E+00 5.311E+00 5.278E+00 5.246E+00
5.213E+00 5.180E+00 5.147E+00 5.115E+00 5.082E+00 5.049E+00
5.060E+00 5.071E+00 5.082E+00 5.093E+00 5.104E+00 5.115E+00
5.126E+00 5.136E+00 5.147E+00 5.158E+00 5.169E+00 5.180E+00
4.996E+00 4.618E+00 4.240E+00 3.861E+00 3.483E+00 3.105E+00
2.726E+00 2.348E+00 1.969E+00 1.591E+00 1.213E+00 8.344E-01
4.560E-01 4.195E-01 3.830E-01 3.465E-01 3.101E-01 2.736E-01
2.371E-01 2.006E-01 1.642E-01 1.277E-01 9.120E-02 5.472E-02
1.824E-02 0. /
0. 0. 1. 0./
0/
-400/
-500/
-600/
-700/
-800/
-1000/
-1200/
-1600/

```

-2000/
-3000/
' graphite IKE          EVAL-      Keinert, Mattes '/'
' IKE-                  DIST-jan05 Mattes '/'
'----- IAEA-IKE       MATERIAL 31 '/'
'----- THERMAL NEUTRON SCATTERING DATA '/'
'----- ENDF-6 '/'
' '/'
'*-----* '/'
'* Temperatures (K) = 293.6, 400, 500, 600, 700, 800, 1000,      * '/'
'*                   1200, 1600, 2000, 3000                    * '/'
'*                   * '/'
'*-----* '/'
'* generated with LEAPR/NJOY-99.90++                          IKE jan2005 * '/'
'-----' '/'
' '/'
' This evaluation (ref.1) is based on the physical model used at GA'/'
' (see ref. 2) using the LEAPR code (ref. 3) '/'
' Tighter grids for alpha and beta were used. '/'
' The various constants agree with the ENDF/B-VI evaluation of '/'
' natural carbon.'/'
' '/'
' References '/'
' ----- '/'
' 1. M.Mattes, J.Keinert, Status of thermal neutron scattering data '/'
'    for Graphite, july 2005.'/'
' 2. J.U.Koppel and D.H.Houston, Reference Manual for ENDF Thermal '/'
'    Neutron Scattering Data, General Atomic Report GA-8774 '/'
'    revised and reissued as ENDF-269 by the National Nuclear '/'
'    Data Center, july 1978. '/'
' 3. R.E.MacFarlane, New Thermal Neutron Scattering Files for '/'
'    ENDF/B-VI Release 2, LA-12639-MS (aug.1994). '/'
' '/'
/
-- -----end leapr -----
stop

```

b) MCNP Data Sets for Graphite

The NJOY processing code system was used to create for graphite $S(\alpha,\beta,T)$ tables for MCNP from the evaluation based on the GA-model for 11 temperatures from 293 K up to 3000K. NJOY version 99.90 with additional updates particular for the modules THERMR and ACER as reported in the appendix of [2] was used.

The maximum incident neutron energy is 4.46 eV. Information about these data sets - similar to that contained in Appendix G of the MCNP manual - is provided in the following Table. Note that these data sets may be used with any version of MCNP(X). Given in parenthesis are the nuclides for which the $S(\alpha,\beta,T)$ data are valid. In the case of graphite this can be natural carbon or the isotope ^{12}C .

Table App.1 MCNP Data Sets in the *SAB-IKE-2005* Library

Graphite (6000, 6012)					
graph.00t	IAEA-IKE-JEFF-3.1	293.6	16	64	coherent
graph.01t	IAEA-IKE-JEFF-3.1	400	16	64	coherent
graph.02t	IAEA-IKE-JEFF-3.1	500	16	64	coherent
graph.03t	IAEA-IKE-JEFF-3.1	600	16	64	coherent
graph.04t	IAEA-IKE-JEFF-3.1	700	16	64	coherent
graph.05t	IAEA-IKE-JEFF-3.1	800	16	64	coherent
graph.06t	IAEA-IKE-JEFF-3.1	1000	16	64	coherent
graph.07t	IAEA-IKE-JEFF-3.1	1200	16	64	coherent
graph.08t	IAEA-IKE-JEFF-3.1	1600	16	64	coherent
graph.09t	IAEA-IKE-JEFF-3.1	2000	16	64	coherent
graph.10t	IAEA-IKE-JEFF-3.1	3000	16	64	coherent

The **first column** of the Table contains the Z Aid, which is the data set identification to be specified on MCNP(X) MTn cards. The portion of the Z Aid before the decimal point provides a shorthand alphanumeric description of the material. The two digits after the decimal point differentiate among different data sets (different temperatures) for the same material. The final character in the Z Aid is a "t" which indicates thermal $S(\alpha,\beta)$ table.

The **second column** of the Table is the evaluated source file. For this MCNP(X) library, all data are from the IAEA/IKE evaluations, which was accepted for JEFF-3.1.

The **third column** is the temperature of the data (in degrees Kelvin).

The **fourth column** contains the number of equally-likely discrete secondary cosines provided at each combination of incident and secondary energy for inelastic scattering, and for each incident energy for incoherent elastic scattering.

The **fifth column** gives the number of secondary energies provided for each incident energy for inelastic scattering.

There are three options for the elastic scattering entry in the **seventh column**:

- none - no elastic scattering data for this material.
- coherent - coherent elastic scattering data provided for this material (Bragg scattering).
- incoh - incoherent elastic scattering data provided for this material.

The associated xsdir file for the generated ACE-library *graphit.ace* is given below.

xsdir

```

directory
graph.00t 11.898000 graphit.ace 0 1 1 85354 0 0 2.5301E-08
graph.01t 11.898000 graphit.ace 0 1 21352 85326 0 0 3.4470E-08
graph.02t 11.898000 graphit.ace 0 1 42696 85308 0 0 4.3087E-08
graph.03t 11.898000 graphit.ace 0 1 64035 85292 0 0 5.1704E-08
graph.04t 11.898000 graphit.ace 0 1 85370 85282 0 0 6.0322E-08
graph.05t 11.898000 graphit.ace 0 1 106703 85268 0 0 6.8939E-08
graph.06t 11.898000 graphit.ace 0 1 128032 85240 0 0 8.6174E-08
graph.07t 11.898000 graphit.ace 0 1 149354 85218 0 0 1.0341E-07
graph.08t 11.898000 graphit.ace 0 1 170671 85194 0 0 1.3788E-07
graph.09t 11.898000 graphit.ace 0 1 191982 85182 0 0 1.7235E-07
graph.10t 11.898000 graphit.ace 0 1 213290 85144 0 0 2.5852E-07

```

The temperature dependent total neutron cross sections for graphite as given in the MCNP(X) library are shown in the Figure below.

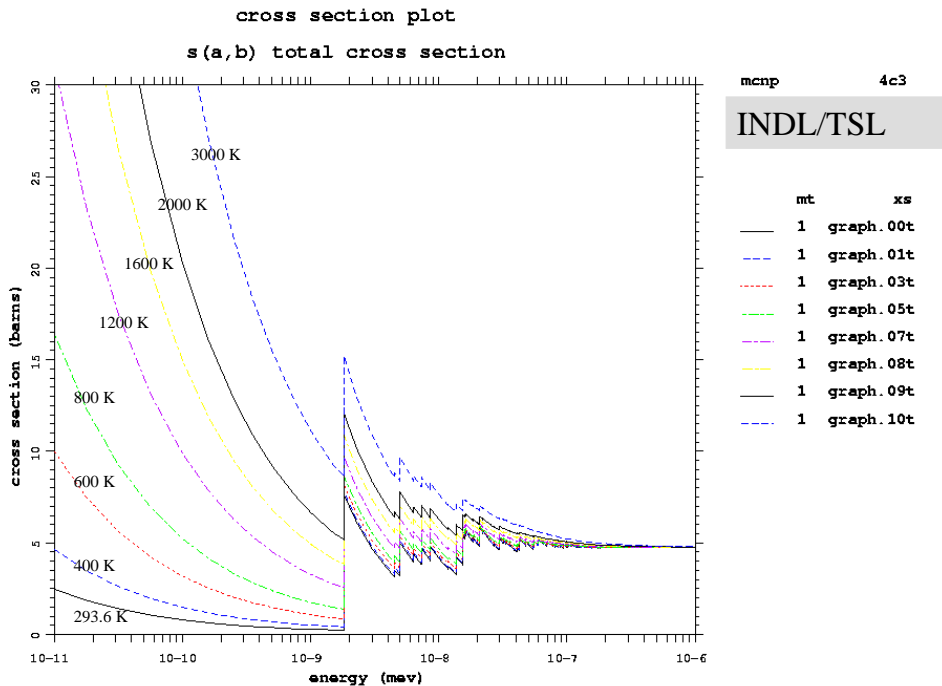


Figure App.1 Total neutron cross section for graphite as a function of temperature, data are based on the GA frequency distribution.

Nuclear Data Section
International Atomic Energy Agency
P.O. Box 100
A-1400 Vienna
Austria

e-mail: services@iaeand.iaea.org
fax: (43-1) 26007
telephone: (43-1) 2600-21710
Web: <http://www-nds.iaea.org>
